HHS Public Access

Author manuscript

Am J Transplant. Author manuscript; available in PMC 2022 October 01.

Published in final edited form as:

Am J Transplant. 2021 October ; 21(10): 3256–3267. doi:10.1111/ajt.16571.

TIGIT regulates apoptosis of risky memory T cell subsets implicated in belatacept-resistant rejection

He Sun[1,2], **Christina R. Hartigan**[1], **Ching-wen Chen**[1], **Yini Sun**[1,2], **Marvi Tariq**[1], **Jennifer M. Robertson**[1], **Scott M. Krummey**[1], **Aneesh K. Mehta**[1], **Mandy L. Ford**[1]

[1]Emory Transplant Center, Department of Surgery, Emory University School of Medicine, Atlanta, Georgia

[2]Department of Transplant and Hepatobiliary Surgery, The First Hospital of China Medical University, China Medical University, Shenyang, China

Abstract

Belatacept confers increased patient and graft survival in renal transplant recipients relative to calcineurin inhibitors, but is associated with an increased rate of acute rejection. Recent immunophenotypic studies comparing pre-transplant T cell phenotypes of patients who reject vs. those that remain stable on belatacept identified three potential "risky" memory T cell subsets that potentially underlie belatacept-resistant rejection: $CD4^+$ $CD28^+$ T_{EM}, $CD8^+$ $CD28^{null}$ and $CD4^+$ $CD57^+$ $PD1^-$ subsets. Here, we compared key phenotypic and functional aspects of these human memory T cell subsets, with the goal of identifying additional potential targets to modulate them. Results demonstrate that TIGIT, an increasingly well-appreciated immune checkpoint receptor, was expressed on all three risky memory T cell subsets *in vitro* and *in vivo* in the presence of belatacept. Co-culture of human memory $CD4^+$ and $CD8^+$ T cells with an agonistic anti-TIGIT mAb significantly increased apoptotic cell death of all three risky memory T cell subsets. Mechanistically, TIGIT-mediated apoptosis of risky memory T cells was dependent on $FOXP3^+$ Treg, suggesting that agonism of the TIGIT pathway increases $FOXP3^+$ Treg suppression of human memory T cell populations. Overall, these data suggest that TIGIT agonism could represent a new therapeutic target to inhibit belatacept-resistant rejection during transplantation.

Corresponding Author: Mandy L. Ford, mandy.ford@emory.edu.

Author Contributions

He Sun: Formal analysis, Investigation, Writing-original draft
Christina R. Hartigan: Formal analysis, Investigation, Writing-review & editing
Ching-wen Chen: Investigation, Writing-review & editing
Yini Sun: Investigation, Writing-review & editing
Marvi Tariq: Blood withdrawals, Assistance with flow cytometry and in vitro stimulation assay, Writing-review & editing
Jennifer M. Robertson: Panel design, Blood withdrawals, Assistance with flow cytometry, Writing-review & editing
Scott M. Krummey: Blood withdrawals, Writing-review & editing
Aneesh K. Mehta: Writing-IRB protocol, PI of IRB
Mandy L. Ford: Conceptualization, Formal analysis, Funding acquisition, Project administration, Supervision, Writing-review & editing

Disclosure

The authors of this manuscript have no conflicts of interest to disclose as described by the *American Journal of Transplantation*.

Supporting information

Additional supporting information may be found online in the Supporting Information section at the end of the article.

Introduction

Transplantation is a curative, life-saving therapy for end-stage organ failure. However, the incidence of significant morbidity and graft loss due to immunosuppression-induced toxicities remains unacceptably high (1, 2). CD28 costimulation blockade in the form of belatacept is a CTLA-4Ig fusion protein and the first new primary immunosuppressive agent in transplantation in over 20 years (3, 4). Belatacept offers a significant benefit to renal transplant recipients in that it carries a 43% reduced risk of death or graft loss after 7 years as compared to calcineurin inhibitor-based regimens (5). Nonetheless, belatacept confers a significantly increased risk of acute rejection as compared to calcineurin inhibitors (6–8), a fact that has limited its uptake in the clinical transplant community. Our work and that of many others has revealed that belatacept-resistant rejection is likely the result of the activation of memory T cells that have a diminished requirement for CD28 signaling (9–12). The resistance of memory T cells to the effects of costimulatory blockade may therefore markedly limited patient access to the considerable benefits of belatacept.

To optimize the potential of belatacept in clinical transplantation, several groups have endeavored to identify “risky” memory T cell phenotypes that may predict the development of belatacept-resistant rejection. First, it has been hypothesized that $CD28^{null}$ $CD4^{+}$ and $CD8^{+}$ T cell populations contribute to belatacept-resistant rejection, owing to their lack of expression of the target of belatacept (3, 4) and the fact that patients with kidney failure awaiting transplantation have been described to accumulate $CD28^{null}$ cells in peripheral blood (13, 14). However, whether these cells are functionally capable of mediating belatacept-resistant rejection remains a topic of ongoing debate in the field (15–17). In contrast, our previous findings suggest that patients possessing higher frequency of $CD28^{+}$ $CD4^{+}$ T_{EM} prior to transplant are more likely to experience acute rejection following treatment with a belatacept-based immunosuppressive regimen, and pre-transplant frequencies of $CD28^{+}$ $CD4^{+}$ T_{EM} have the potential to be used as a biomarker to predict the risk of rejection following treatment with belatacept (18). Further, a population of $CD57^{+}$ $PD1^{-}$ $CD4^{+}$ T cells present prior to transplantation has also been reported to correlate with belatacept-resistant rejection, and likewise this immunophenotype has been proposed to identify patients at higher risk for acute rejection on belatacept-based therapy (19). The similarities and differences, as well as potential overlap, between these memory T cell subsets has not been investigated. Moreover, identification of molecules and pathways that regulate their activation and functionality in the setting of CD28 blockade remains an important goal for immunotherapy in clinical transplantation.

The T cell immunoreceptor with Ig and ITIM domains (TIGIT) has recently been identified as an important immune checkpoint receptor. TIGIT is a CD28 family member (20, 21) that pairs with DNAM (CD226) to form an increasingly well-appreciated cosignaling pathway: DNAM and TIGIT compete for binding to the same set of ligands (CD155 and CD112), but TIGIT is coinhibitory for T cells while DNAM is costimulatory (22, 23). These relationships are analogous to the CD28/ CTLA-4/ CD80/ CD86 family of costimulatory/ coinhibitory molecules.

TIGIT can inhibit T cell responses by binding the ligand CD155 on DCs and thereby inhibiting IL-12 while inducing IL-10 production, resulting in a cell-extrinsic mechanism of inhibition of T cell responses (24, 25). Furthermore, recent studies have revealed that TIGIT expression defines a population of highly suppressive regulatory T cells (T_{reg}) in both mouse and humans (20, 26, 27), and contributes to the selective T_{reg} cell-mediated suppression of pro-inflammatory Th1 and Th17 cells but not Th2 responses (27). Importantly, TIGIT is currently being targeted therapeutically in several ongoing clinical trials in cancer (28–31) (#NCT02794571, #NCT03119428, #NCT03628677 ClinicalTrials.gov). However, the role of TIGIT signaling in regulating alloreactive immune responses, especially these risky memory T cell subsets implicated in belatacept-resistant rejection in the context of solid organ transplantation has not been fully elucidated. Furthermore, the ability of TIGIT to inhibit memory/effector T cells in a cell-intrinsic fashion remains controversial. For instance, in a naïve mouse tumor model, TIGIT primarily suppressed $CD8^+$ antitumor immunity via T_{reg} cells and not a cell-autonomous effect on $CD8^+$ T cells (32). Conversely, TIGIT has also been reported to directly regulate the expansion and function of tumor antigen-specific $CD8^+$ T cells in vitro in the absence of T_{reg} (33).

Here, we endeavored to define the expression of TIGIT on risky human memory T cell subsets associated with belatacept-resistant rejection, and show that TIGIT agonism attenuates risky memory T cell responses by increasing apoptotic cell death in a $FOXP3^+$ Treg-dependent fashion.

Materials and Methods

Human study approval, sample collection, and patient immunosuppression

PBMCs were collected from healthy volunteers and renal transplant patients treated with belatacept following protocols approved by the Emory University Institutional Review Board (IRB #00006248) after informed consent was obtained. Patients treated with belatacept received intravenous infusion of belatacept (10mg/kg) during surgery and on post-transplant days 28, 56, and 84 with subsequent doses (5mg/kg) given every 4 weeks thereafter. Belatacept-treated patients also received anti-IL-2R induction (basiliximab 20mg iv on days 0 and 3 or 4), mycophenolate mofetil (MMF, 1g twice daily), a short steroid taper (methylprednisolone 500mg iv intra-operatively, 250 mg iv d1, 125mg iv d2, and prednisone 5mg d3 and daily thereafter), and a tacrolimus taper over the first 3-9 months (target trough levels 5-12ng/ml) as previously described (8). Patients who were Epstein Barr virus (EBV) seronegative, HIV^+, had a history of post-transplant lymphoproliferative disease (PTLD), lymphoma or other hematologic malignancy, were undergoing treatment for latent tuberculosis or were the recipient of a simultaneous extra-renal organ were excluded from belatacept treatment. PBMC were obtained from patients who were stable on belatacept 6-12 months post-transplantation. Pre-transplant samples (n=5) consisted of 4 males and 1 female, average age 54.0 (range 44-63), 60% Black and 40% White, and underlying disease of diabetes mellitus (DM) (n=3), hypertension (n=1), and FSGS (n=1). Post-transplant samples (n=7) consisted of 6 males and 1 female, average age 54.4 (range 41-72), 57.1% Black, 28.6% White, and 14.4% American Indian or Alaskan Native; and underlying disease

of DM (n=2), hypertension (n=4), and familial nephropathy (n=1). None of the pre- vs. post-transplant samples were from the same donor.

Ex vivo analysis of T cell phenotype and apoptosis

Standard extracellular staining (20 mins at 24°C) was performed using the following fluorophore-labeled antibodies: CD3-BUV737 (BD Biosciences), CD4-BUV395 (BD Biosciences), CD8-BV711 (BD Biosciences), CD14-BV510 (BD Biosciences), CD19-BV510 (BioLegend), Live/Dead Fixable Aqua (ThermoFisher), CCR7-PE-CF594 (BD Biosciences), CD45RA-APC-H7 (BD Biosciences), CD28-APC-R700 (BD Biosciences), CD57-PE (BioLegend), PD-1-BV605, BV421 (BioLegend), CD69-BV650 (BioLegend), CD38-BV421 (BioLegend), HLA-DR-PerCP-Cy5.5 (BD Biosciences), TIGIT-PE-Cy7 (BioLegend), DNAM-BB515 (BD Biosciences), FcγRIIB-BV786 (BD Biosciences). Fluorescence minus one (FMO) controls were used to determine negative expression of FcγRIIB. Apoptosis was measured with Caspase-3/7 Green Flow Cytometry Assay Kit (ThermoFisher) or FITC Annexin V with 7-AAD Viability Staining Solution (BioLegend), according to the manufacturer's instructions.

Ex vivo polyclonal stimulation assay

Fresh PBMCs were isolated from healthy donors under IRB approval using CPT tubes and incubated in 24-well flat-bottomed plates in culture medium (R10) consisting of 1640 RPMI medium supplemented with 10% heat-inactivated FBS (Mediatech, Herdon, VA), 1% L-glutamine (200mM), 1% penicillin/streptomycin (100×), 1% Hepes (1M), 1% 2-ME (5mM). Cells were processed unstimulated, stimulated with anti-CD3/CD28 Dynabeads (ThermoFisher) per manufacturer instructions, or stimulated with 3 μg/mL plate-bound functional grade anti-CD3 (OKT3; eBiosciences) with clinically therapeutic concentrations of belatacept (10 μg/mL; Bristol-Myers Squibb, NY) (34, 35) for 3 days at 37°C and 5% CO_2, humidified atmosphere. Where indicated, cultures were treated with 10 μg/mL LPS- and azide-free agonistic αTIGIT (A15153G; BioLegend) or mouse IgG2a isotype control (MOPC-173; BioLegend). Where indicated, cultures were washed twice with media and restimulated with 50 ng/mL PMA (Sigma) and 1 μg/mL Ionomycin (Sigma) in the presence of GolgiStop (BD Biosciences) for 4 h at 37°C, 5% CO_2. Where indicated, conventional $CD4^+$ or $CD8^+$ T cells or $CD25^+$ Treg were purified by MACS according to the manufacturer's instructions (Miltenyi Biotech).

Alloreactive proliferation assay

One-way mixed lymphocyte reactions (MLRs) were performed using human PBMCs from 8 stimulator-responder pairs. Irradiated stimulator PBMCs (8×10^5) were labeled with CellTrace Violet dye (CTV, ThermoFisher) with 1 μL of 5mM CTV per 10^7 cells at RT for 20 minutes, and then cultured with responder PBMCs (4×10^5) in culture medium R10 as described above with 10% plasma from the responders for 6 days at 37°C in a 5% CO_2, humidified atmosphere. Where indicated, cultures were treated with 10 μg/mL LPS- and azide-free agonistic αTIGIT or isotype control in the presence or absence of belatacept.

Ex vivo intracellular cytokine staining

Cells were cultured in round-bottom 96-well plates in R10 media. PMA/Ionomycin and Golgi Stop were also added for 4 hours as described above at 37°C, 5% CO_2. Intracellular staining was performed after fixation and permeabilization using FOXP3 Staining Buffer Set (eBioscience) according to manufacturer's instructions, utilizing fluorophore-labeled antibodies to Ki-67-FITC (BD Biosciences), Foxp3-APC (eBioscience), IL-2-BV605 (BioLegend), IFN-γ-BV785 (BioLgend), TNF-BV650 (BioLegend), IL-17-APC-R700 (BD Biosciences) following extracellular staining as described above. Samples were acquired on a Fortessa flow cytometer (BD Biosciences), and data were analyzed using FlowJo software (9.9.6 FlowJo, LLC) and GraphPad Prism Version 7.

Statistics

Data shown and described depict the mean ± SEM. T cell responses were analyzed using paired, nonparametric, Wilcoxon matched-pairs signed-rank test. All statistical analyses were conducted using GraphPad Prism 7.0 software (San Diego, CA). Significance was determined as *$p < 0.05$, **$p < 0.005$. All calculated p values were two-tailed analyses.

Results

$CD4^+$ $CD28^+$ T_{EM} subset exhibits high proliferative capacity and cytokine functionality and low frequencies of apoptotic cells following stimulation with alloantigen

To compare phenotypic and functional characteristics of the three "risky" memory T cell subsets associated with belatacept-resistant rejection, human PBMCs were isolated from healthy volunteers, ranging in age from 28 to 63. Responder PBMCs were cultured alone or in the presence of irradiated, CTV-labeled, allogeneic stimulator PBMCs. Subsets were analyzed for proliferation, apoptosis, and cytokine production using flow cytometry. Gating strategies to identify the "risky" memory T cell subsets previously identified as being associated with belatacept-resistant rejection are depicted in Supplemental Figure 1. As depicted in Figure 1A, the $CD4^+$ $CD28^+$ T_{EM} subset contained higher frequencies of alloantigen-driven Ki-67^+ proliferating cells upon allogeneic stimulation as compared to the $CD8^+$ $CD28^{null}$ subset (the $CD4^+$ $CD57^+$ $PD1^-$ subset exhibited a similar trend). We next queried the frequencies of apoptotic cells within risky memory T cell subsets in allogeneic co-cultures. Within the responder alone cultures, the $CD4^+$ $CD57^+$ $PD1^-$ subset contained a significantly higher frequency of Caspase $3/7^+$ 7-AAD^+ apoptotic cells following ex vivo culture relative to the other two subsets (Figure 1B). Following culture with allogeneic stimulators, both the $CD4^+$ $CD57^+$ $PD1^-$ subset and the $CD8^+$ $CD28^{nul}$ subset contained significantly increased frequencies of Caspase $3/7^+$ 7-AAD^+ apoptotic cells relative to the $CD4^+$ $CD28^+$ T_{EM} subset (Figure 1B). The cytokine-producing functionalities of three risky memory T cell subsets were then evaluated. $CD4^+$ $CD28^+$ T_{EM} and $CD4^+$ $CD57^+$ $PD1^-$ subsets yielded increased frequencies of TNF and IFN-γ producers compared to $CD8^+$ $CD28^{null}$ subset (Figure 1C). Results for polyclonal stimulations using anti-CD3/CD28 beads as described in the Materials and Methods exhibited similar trends (Supplemental Figure 2). Collectively, these data demonstrate that the $CD4^+$ $CD28^+$ T_{EM} subset exhibits the most proliferative capacity combined with the least death relative to the other two subsets, while retaining strong functional capacity.

CD4+ CD28+ T_{EM} and CD4+ CD57+ PD1− subsets exhibit high CD69 upregulation and CD4+ CD28+ T_{EM} exhibit high CD38 and HLA-DR upregulation following stimulation

We next sought to evaluate the expression profile of activation markers on risky memory T cell subsets. CD69, one of the earliest T cell activation markers, was significantly increased within $CD4^+$ $CD28^+$ T_{EM} and $CD4^+$ $CD57^+$ $PD1^-$ subsets upon stimulation (Figure 2A–B). In contrast, expression of the activation markers CD38 and HLA-DR were upregulated on $CD4^+$ $CD28^+$ T_{EM} subset but not on $CD4^+CD57^+PD\text{-}1^-$ or $CD8^+$ $CD28^{null}$ cells following stimulation (Figure 2C–D).

We hypothesized that there might be potential overlap between these risky memory T cell subsets. To investigate this possibility, we utilized viSNE analysis from the Cytobank platform (Cytobank.org). viSNE is an algorithm which employs t-stochastic neighbor embedding (t-SNE) to reduce high-dimensional cytometry data down to a two-dimensional map for ease of visualization, where the distance between cells corresponds to their marker profile similarity. Color is then used as a third dimension to interactively visualize features of these cells (36). When the profiles of the gated $CD4^+$ T cells were visualized by viSNE, the resulting viSNE maps clearly distinguished $CD4^+$ $CD28^+$ T_{EM} vs. $CD4^+$ $CD57^+$ $PD1^-$ populations in space (depicted as red-rimmed and the purple-rimmed islands, respectively, in Figure 2E). Interestingly, results demonstrated minimal overlap between the two populations. Summary data of CD57, PD-1 and CD28 expression on the three memory T cell subsets revealed that $CD4^+$ $CD28^+$ T_{EM} subset exhibited the lowest expression of CD57 (less than 10%), and the highest expression of PD-1 (roughly 40%) among all the risky memory T cell subsets (Figure 2F). We also found that $CD4^+$ $CD57^+$ $PD1^-$ subset was composed predominantly of T_{EM} and T_{EMRA} subsets (Figure 2E) and the CD28 expression on $CD4^+$ $CD57^+$ $PD1^-$ subset was extremely variable (from 3% to 97%) (Figure 2F). In directly analyzing the overlap between the subsets, we found that only ~0.6% of $CD4^+$ $CD4^+$ $CD28^+$ T_{EM} were $CD57^+$ $PD\text{-}1^-$ cells. Likewise, ~14% of $CD4^+$ $CD57^+$ $PD\text{-}1^-$ cells were $CD4^+$ $CD28^+$ T_{EM} (Figure 2G–H). Thus, $CD4^+$ $CD28^+$ T_{EM} and $CD4^+$ $CD57^+$ $PD1^-$ subsets exhibit minimal overlap, and thus they may play distinct and non-redundant roles in mediating belatacept-resistant rejection.

TIGIT expression is maintained on “risky” memory T cell subsets in vivo and in vitro in the presence of belatacept

Given the finding that these T cell populations may be non-overlapping and therefore play non-redundant roles in mediating belatacept-resistant rejection, we aimed to identify coinhibitory receptors expressed on all three subsets that could potentially be targeted to limit their response following transplantation. As depicted in Figure 3A–B, all three memory T cell subsets expressed the coinhibitory molecule TIGIT. While TIGIT expression increased on all subsets following stimulation (Supplemental Figure 3A), the $CD8^+$ $CD28^{null}$ subset exhibited the highest level of TIGIT expression both pre- and post- anti-CD3 stimulation as compared to the $CD4^+$ $CD28^+$ T_{EM} or $CD4^+$ $CD57^+$ $PD1^-$ subsets. The expression of TIGIT on these three risky memory T cell subsets in comparison to naïve, central memory, and effector memory $CD4^+$ and $CD8^+$ T cell subsets is shown in Supplemental Figure 3B–C. In contrast, the $CD8^+$ $CD28^{null}$ subset showed significantly

lower expression of the costimulatory counter-receptor DNAM in both pre- and post-stimulation samples relative to the other two subsets (Figure 3C).

We next investigated TIGIT expression on memory T cell subsets following stimulation in the setting of belatacept. Following polyclonal stimulation with plate-bound anti-CD3 and CD80/CD86-expressing APC in the presence of belatacept, TIGIT and DNAM were both still expressed on all three risky memory T cell subsets (Figure 3D–E, Supplemental Figure 3D). In the presence of belatacept, there were no statistically significant differences in TIGIT expression between the three subsets. Intriguingly, belatacept resulted in a statistically significant increase in TIGIT expression on $FOXP3^+$ Treg (Supplemental Figure 3E). These data therefore suggest that TIGIT could be a therapeutic target on all three risky memory T cell subsets in the context of belatacept therapy.

To assess the in vivo expression patterns of TIGIT and DNAM in renal transplant patients treated with belatacept, peripheral T cells from renal transplant recipients treated with belatacept (as described in (8)) were analyzed directly at baseline or following transplantation (Figure 3F–G). Consistent with the in vitro data, all three memory T cell subsets isolated ex vivo from belatacept-treated renal transplant recipients expressed TIGIT and DNAM. These results suggest that while expression patterns of TIGIT and DNAM may indicate the $CD8^+$ $CD28^{null}$ subset is more exhausted and/or senescent relative to the other two subsets, TIGIT is still maintained on all the three risky memory T cell subsets *in vivo* and *in vitro* in the presence of belatacept.

Agonistic αTIGIT induces apoptosis in all three “risky” memory T cell subsets both in the presence and absence of belatacept

We next sought to determine whether agonism of the TIGIT pathway could inhibit responsiveness of these “risky” memory T cell subsets associated with belatacept-resistant rejection. Responder PBMCs were stimulated ex vivo with allogeneic antigens and treated with a TIGIT-specific agonistic monoclonal antibody (clone: A15153G) or isotype control. Relative to isotype control, there were no differences in the frequency of Ki-67^+ proliferating cells among any of the three subsets in the presence or absence of belatacept (Supplemental Figure 4A), indicating that TIGIT agonism does not inhibit proliferation of these memory T cell subsets. Similarly, TIGIT agonism failed to modulate TNF, IFN-γ and IL-2 production on risky memory T cell subsets (Supplemental Figure 4B–D). However, as depicted in Figure 4, significant increases in apoptosis as measured by Caspase $3/7^+$ 7-AAD^+ double positive cells were observed in the presence of agonistic αTIGIT in all the three risky memory T cell subsets, indicating that TIGIT agonism results in increased cell death among all three risky memory T cell subsets associated with belatacept-resistant rejection. Indeed, TIGIT agonism in the presence of belatacept also resulted in markedly increased frequencies of active Caspase $3/7^+$ 7-AAD^+ cells among all three risky memory T cell subsets (Figure 4A–B). These data therefore demonstrate that TIGIT agonism results in the attenuation of risky memory T cell responses by increasing apoptotic cell death.

TIGIT-mediated memory T cell apoptosis requires FOXP3$^+$ Treg

As shown above, TIGIT agonism resulted in increased apoptosis in belatacept-resistant CD4$^+$ and CD8$^+$ memory T cell responses. Because these cultures were performed using PBMC that contained T_{reg}, and because Treg contain high frequencies of TIG IT$^+$ cells (Supplemental Figure 5A), it was unclear whether the effect of TIGIT agonism on memory T cell apoptosis was a cell-autonomous effect, or due to TIGIT agonism-mediated activation of FOXP3$^+$ T_{reg} in these cultures (27, 32). To determine the ability of TIGIT agonism to induce risky memory T cell apoptosis in a cell-autonomous manner, CD25$^-$ CD4$^+$ T_{conv} and CD8$^+$ T cells were sorted such that all cultures were devoid of FOXP3$^+$ Treg, and stimulated ex vivo with anti-CD3/CD28 beads in the presence or absence of agonistic αTIGIT (Figure 5A). Analysis of Caspase 3/7 and 7-AAD staining revealed that TIGIT agonism was ineffective at inducing apoptosis in sorted risky memory T cell subsets in the absence of FOXP3$^+$ regulatory T cells (Figure 5B–C), compared to the effect of TIGIT agonism when FOXP3$^+$ Treg were present (Figure 4). Moreover, “adding back” increasing numbers of FOXP3$^+$ Treg to purified CD4$^+$ or CD8$^+$ memory T cell populations resulted in increased frequencies of apoptotic cells in cultures treated with the anti-TIGIT agonist, but not cultures treated with isotype control (Supplemental Figure 5B–E). These data therefore demonstrate that although all memory T cell subsets express TIGIT, the presence of FOXP3$^+$ Treg is required for the TIGIT agonist to mediate its suppressive effect on these cells.

Discussion

Identifying strategies to overcome belatacept-resistant rejection may allow more renal transplant recipients to benefit from the improved toxicity profile of belatacept relative to standard CNI-based immunosuppression (1, 2, 5). In the present study, we show that TIGIT is expressed on three risky memory T cell subsets that have been previously implicated in belatacept-resistant rejection (15, 18, 19), and that TIGIT agonism functions to inhibit human risky memory T cell responses in the presence of belatacept by inducing apoptotic cell death. The finding that TIGIT coinhibition may inhibit memory T cell alloreactivity by exclusively increasing apoptosis (as opposed to limiting cellular proliferation or effector function) is somewhat unique among T cell coinhibitory pathways. For example, CTLA-4 coinhibitory signaling has been identified to regulate cell cycle progression, but does not effectively impact cell death (37–39). Engagement of PD-1 signaling can block T cell proliferation, cytokine production and cytolytic function, and also impair T cell survival (40, 41). PD-1 coinhibition is also known to inhibit cytokine production to a greater extent than cell proliferation. Here, our study provides insight into the biologic role of TIGIT agonism in modulating risky memory T cell response and demonstrates that TIGIT signaling regulates risky memory T cell apoptotic cell death, but does not differentially affect the proliferation and effector function of risky memory T cell subsets.

Our results further demonstrate that the ability of TIGIT agonism to induce risky memory T cell apoptosis requires FOXP3$^+$ Treg. There are two main paradigms to explain these findings. First, it is possible that the TIGIT agonist induces a negative signal directly into the memory T cell but requires some factor from FOXP3$^+$ Treg, such as IL-10, TGF-beta, or even the removal of CD28-mediated costimulation, to push memory T cells to undergo

apoptosis. The second possibility is that the TIGIT expressed on memory T cells themselves is not at all required for apoptosis, but that agonism of TIGIT on FOXP3$^+$ Treg results in Treg-mediated induction of apoptosis of memory T cells. The main differentiating factor between these two scenarios is the requirement for TIGIT to be expressed on the memory T cell in order for the TIGIT agonist to mediate the apoptosis-inducing effect. Evidence supporting both paradigms exists in the literature. For example, Chauvin et al. found that TIGIT was upregulated on CD8$^+$ tumor-infiltrating lymphocytes (TIL), and in vitro culture experiments suggested that TIGIT blockade was functioning directly on effector/ memory T cells in a cell intrinsic manner, and not through the activation or stabilization of Foxp3$^+$ Treg (33). Joller et al. reported similar findings in in vitro cultures of CNS-specific memory T cells (42) and Josefsson et al. showed that TIGIT expression correlated with dysfunctional TCR signaling in effector/memory CD8$^+$ T cells in human anti-tumor responses. On the other hand, a myriad of studies have identified an indirect role for TIGIT in inhibiting effector T cell responses, via an effect on a Treg intermediate. For instance, TIGIT agonism has been shown to augment Foxp3$^+$ Treg suppressive function (27), and TIGIT$^+$ T cells can induce immunoregulatory DC via ligation of CD155 (24, 30, 43). Conditional knockout studies in mice, or knockdown studies of human T cells, will be required to definitively determine the cell autonomous role of TIGIT signaling on belatacept-resistant memory T cell subsets.

Data presented here also depict a direct comparison of the phenotypic and functional profiles of the three memory T cell subsets known to be associated with belatacept-resistant rejection. These analyses show that the CD4$^+$ CD28$^+$ T_{EM} subset was on par with CD4$^+$ CD57$^+$ PD1$^-$ subset in terms of proliferative capacity, activation (CD69) and pro-inflammatory cytokine production (TNF, IFN-γ, IL-2) upon stimulation. Likewise, similar expression patterns of TIGIT and DNAM were noted on CD4$^+$ CD28$^+$ T_{EM} and CD4$^+$ CD57$^+$ PD1$^-$ subsets. Thus, we conclude that the CD4$^+$ CD28$^+$ T_{EM} and CD4$^+$ CD57$^+$ PD1$^-$ subsets are more similar to each other than either is to the CD8$^+$ CD28^{null} subset. While these subsets may be functionally similar, viSNE analysis showed that the cell populations themselves are non-overlapping, raising the possibility that they could play non-redundant roles in mediating belatacept-resistant rejection. Importantly, while CD4$^+$ CD57$^+$ PD1$^-$ cells readily underwent apoptosis following allogeneic stimulation, CD4$^+$ CD28$^+$ T_{EM} cells were relatively resistant to apoptosis. These data suggest that increasing apoptosis of CD4$^+$ CD28$^+$ T_{EM} cells, potentially through the TIGIT pathway, could be an effective method to control their response.

To our knowledge, there is only one report comparing these three signatures of risky memory T cell subsets in terms of their association with belatacept-resistant rejection (44). As part of a clinical trial, pretransplant frequencies of these risky memory T cell subsets in belatacept-treated renal transplant patients (n=20) were analyzed. Only the pre-transplant frequency of CD8$^+$ CD28^{++} T_{EMRA} trended toward an increase in patients who underwent belatacept-resistant rejection as compared to those that remained stable, suggesting that this putative pre-transplant cellular biomarker warrants further investigation. Moreover, continuing to amass more subjects to understand the range of prevalence of these risky memory T cell subsets in both transplant candidates and normal controls is an important goal. In addition, it will be important to understand if these frequencies are

dynamic over time in both healthy controls and transplant patients, in order to determine the stability of this potential biomarker. While this study examined the association between belatacept-resistant rejection and $CD8^+$ $CD28^+$ T_{EMRA} instead of $CD4^+$ $CD28^+$ T_{EMRA}, it is worth noting that we also showed that TIGIT agonism induced apoptotic cell death of $CD8^+$ $CD28^+$ both T_{EMRA} and T_{EM} subsets (Supplemental Figure 4). While we have certainly identified differences between the three human memory T cell subsets associated with belatacept-rejection, it is also interesting that all three subsets behaved similarly in response to TIGIT-mediated inhibition: that is, TIGIT coinhibition induced cell death but did not inhibit proliferation or effector function in all three subsets, and in all three subsets were $FOXP3^+$ Treg required for the apoptosis-inducing effects of TIGIT coinhibition. These results demonstrate that despite their phenotypic and functional differences, TIGIT coinhibition exacts a similar impact on all memory T cell subsets associated with belatacept-resistant rejection, suggesting that therapeutic targeting of this pathway would have a rather homogeneous and predictable effect on belatacept-resistant memory T cell responses.

In conclusion, agonism of the TIGIT coinhibitory pathway regulates the apoptosis of risky memory T cell subsets associated with belatacept-resistant rejection. These data increase our fundamental understanding of the role of TIGIT signaling on immunity to allografts, and offer novel insight to inform and direct the translation of TIGIT agonism as a potential new therapeutic target in clinical transplantation.

Supplementary Material

Refer to Web version on PubMed Central for supplementary material.

Acknowledgments

The authors would like to thank the patients, healthy donors and members of the ETC Biorepository for patient sample collection. We would also like to thank Maylene E. Wagener for assistance with immune cell irradiation and Bristol-Myers Squibb for providing belatacept. This work was supported by NIH R01s AI073707 (M.L.F.) and AI104699 (M.L.F.), and the Carlos and Marguerite Mason Trust Foundation.

Data Availability Statement

The data that support the findings of this study are available from the corresponding author upon request.

Abbreviations

APC	antigen-presenting cell
DC	dendritic cell
DNAM	DNAX accessory molecule
FBS	fetal bovine serum
IFN-γ	interferon-γ
IL-2	interleukin-2

IL-17	interleukin-17
PBMC	peripheral blood mononuclear cell
PMA	phorbol 12-myristate 13-acetate
T_{CM}	central memory T cell
T_{EM}	effector memory T cell
T_{EMRA}	effector memory RA T cell
TIGIT	T cell immunoreceptor with Ig and ITIM domains
TNF	tumor necrosis factor
T_{reg}	regulatory T cell

References

1. Hart A, Smith JM, Skeans MA, Gustafson SK, Stewart DE, Cherikh WS, Wainright JL, Kucheryavaya A, Woodbury M, Snyder JJ, et al. OPTN/SRTR 2015 Annual Data Report: Kidney. Am J Transplant. 2017;17 Suppl 1 (21–116. [PubMed: 28052609]
2. Issa N, Kukla A, and Ibrahim HN. Calcineurin inhibitor nephrotoxicity: a review and perspective of the evidence. Am J Nephrol. 2013;37(6):602–12. [PubMed: 23796509]
3. Larsen CP, Elwood ET, Alexander DZ, Ritchie SC, Hendrix R, Tucker-Burden C, Cho HR, Aruffo A, Hollenbaugh D, Linsley PS, et al. Long-term acceptance of skin and cardiac allografts after blocking CD40 and CD28 pathways. Nature. 1996;381(6581):434–48. [PubMed: 8632801]
4. Larsen CP, Pearson TC, Adams AB, Tso P, Shirasugi N, Strobed E, Anderson D, Cowan S, Price K, Naemura J, et al. Rational development of LEA29Y (belatacept), a high-affinity variant of CTLA4-lg with potent immunosuppressive properties. Am J Transplant. 2005;5(3):443–53. [PubMed: 15707398]
5. Vincenti F, Rostaing L, Grinyo J, Rice K, Steinberg S, Gaite L, Moal MC, Mondragon-Ramirez GA, Kothari J, Polinsky MS, et al. Belatacept and Long-Term Outcomes in Kidney Transplantation. N Engl J Med. 2016;374(4):333–43. [PubMed: 26816011]
6. Vincenti F, Larsen C, Durrbach A, Wekerle T, Nashan B, Blancho G, Lang P, Grinyo J, Halloran PF, Solez K, et al. Costimulation blockade with belatacept in renal transplantation. N Engl J Med. 2005;353(8):770–81. [PubMed: 16120857]
7. Vincenti F, Larsen CP, Alberu J, Bresnahan B, Garcia VD, Kothari J, Lang P, Urrea EM, Massari P, Mondragon-Ramirez G, et al. Three-year outcomes from BENEFIT, a randomized, active-controlled, parallel-group study in adult kidney transplant recipients. Am J Transplant. 2012;12(1):210–7. [PubMed: 21992533]
8. Adams AB, Goldstein J, Garrett C, Zhang R, Patzer RE, Newell KA, Turgeon NA, Chami AS, Guasch A, Kirk AD, et al. Belatacept Combined With Transient Calcineurin Inhibitor Therapy Prevents Rejection and Promotes Improved Long-Term Renal Allograft Function. Am J Transplant. 2017;17(11):2922–36. [PubMed: 28544101]
9. Adams AB, Williams MA, Jones TR, Shirasugi N, Durham MM, Kaech SM, Wherry EJ, Onami T, Lanier JG, Kokko KE, et al. Heterologous immunity provides a potent barrier to transplantation tolerance. Journal of Clinical Investigation. 2003;111(12):1887–95.
10. Heeger PS, Greenspan NS, Kuhlenschmidt S, Dejelo C, Hricik DE, Schulak JA, and Tary-Lehmann M. Pretransplant frequency of donor-specific, IFN-gamma-producing lymphocytes is a manifestation of immunologic memory and correlates with the risk of posttransplant rejection episodes. J Immunol. 1999;163(4):2267–75. [PubMed: 10438971]

11. Wu Z, Bensinger SJ, Zhang J, Chen C, Yuan X, Huang X, Markmann JF, Kassaee A, Rosengard BR, Hancock WW, et al. Homeostatic proliferation is a barrier to transplantation tolerance. Nat Med. 2004;10(1):87–92. [PubMed: 14647496]
12. Kitchens WH, Haridas D, Wagener ME, Song M, Kirk AD, Larsen CP, and Ford ML. Integrin antagonists prevent costimulatory blockade-resistant transplant rejection by CD8(+) memory T cells. Am J Transplant. 2012;12(1):69–80. [PubMed: 21942986]
13. Kato M, Ono Y, Kinukawa T, Hattori R, Kamihira O, and Ohshima S. Long time follow up of CD28− CD4+ T cells in living kidney transplant patients. Clin transplant. 2004;18(3):242–6. [PubMed: 15142043]
14. Litjens NH, van Druningen CJ, and Betjes MG. Progressive loss of renal function is associated with activation and depletion of naive T lymphocytes. Clin Immunol. 2006;118(1):83–91. [PubMed: 16257266]
15. Engela AU, Baan CC, Litjens NH, Franquesa M, Betjes MG, Weimar W, and Hoogduijn MJ. Mesenchymal stem cells control alloreactive CD8(+) CD28(−) T cells. Clin Exp Immunol. 2013;174(3):449–58. [PubMed: 24028656]
16. Betjes MG. Clinical consequences of circulating CD28-negative T cells for solid organ transplantation. Transpl Int. 2016;29(3):274–84. [PubMed: 26284456]
17. Weaver TA, Charafeddine AH, Agarwal A, Turner AP, Russell M, Leopardi FV, Kampen RL, Stempora L, Song M, Larsen CP, et al. Alefacept promotes co-stimulation blockade based allograft survival in nonhuman primates. Nat Med. 2009;15(7):746–9. [PubMed: 19584865]
18. Cortes-Cerisuelo M, Laurie SJ, Mathews DV, Winterberg PD, Larsen CP, Adams AB, and Ford ML. Increased Pretransplant Frequency of CD28(+) CD4(+) TEM Predicts Belatacept-Resistant Rejection in Human Renal Transplant Recipients. Am J Transplant. 2017;17(9):2350–62. [PubMed: 28502091]
19. Espinosa J, Herr F, Tharp G, Bosinger S, Song M, Farris AB 3rd, George R, Cheeseman J, Stempora L, Townsend R, et al. CD57(+) CD4 T Cells Underlie Belatacept-Resistant Allograft Rejection. Am J Transplant. 2016;16(4):1102–12. [PubMed: 26603381]
20. Anderson AC, Joller N, and Kuchroo VK. Lag-3, Tim-3, and TIGIT: Co-inhibitory Receptors with Specialized Functions in Immune Regulation. Immunity. 2016;44(5):989–1004. [PubMed: 27192565]
21. Le Mercier I, Lines JL, and Noelle RJ. Beyond CTLA-4 and PD-1, the Generation Z of Negative Checkpoint Regulators. Front Immunol. 2015;6(418. [PubMed: 26347741]
22. Levin SD, Taft DW, Brandt CS, Bucher C, Howard ED, Chadwick EM, Johnston J, Hammond A, Bontadelli K, Ardourel D, et al. Vstm3 is a member of the CD28 family and an important modulator of T-cell function. Eur J Immunol. 2011;41 (4):902–15. [PubMed: 21416464]
23. Tahara-Hanaoka S, Shibuya K, Onoda Y, Zhang H, Yamazaki S, Miyamoto A, Honda S, Lanier LL, and Shibuya A. Functional characterization of DNAM-1 (CD226) interaction with its ligands PVR (CD155) and nectin-2 (PRR-2/CD112). Int Immunol. 2004;16(4):533–8. [PubMed: 15039383]
24. Yu X, Harden K, Gonzalez LC, Francesco M, Chiang E, Irving B, Tom I, Ivelja S, Refino CJ, Clark H, et al. The surface protein TIGIT suppresses T cell activation by promoting the generation of mature immunoregulatory dendritic cells. Nat Immunol. 2009;10(1):48–57. [PubMed: 19011627]
25. Zhang D, Hu W, Xie J, Zhang Y, Zhou B, Liu X, Zhang Y, Su Y, Jin B, Guo S, et al. TIGIT-Fc alleviates acute graft-versus-host disease by suppressing CTL activation via promoting the generation of immunoregulatory dendritic cells. Biochim Biophys Acta Mol Basis Dis. 2018;1864(9 Pt B):3085–98. [PubMed: 29960041]
26. Lozano E, Dominguez-Villar M, Kuchroo V, and Hafler DA. The TIGIT/CD226 axis regulates human T cell function. J Immunol. 2012;188(8):3869–75. [PubMed: 22427644]
27. Joller N, Lozano E, Burkett PR, Patel B, Xiao S, Zhu C, Xia J, Tan TG, Sefik E, Yajnik V, et al. Treg cells expressing the coinhibitory molecule TIGIT selectively inhibit proinflammatory Th1 and Th17 cell responses. Immunity. 2014;40(4):569–81. [PubMed: 24745333]
28. Johnston RJ, Comps-Agrar L, Hackney J, Yu X, Huseni M, Yang Y, Park S, Javinal V, Chiu H, Irving B, et al. The immunoreceptor TIGIT regulates antitumor and antiviral CD8(+) T cell effector function. Cancer Cell. 2014;26(6):923–37. [PubMed: 25465800]

29. Dougall WC, Kurtulus S, Smyth MJ, and Anderson AC. TIGIT and CD96: new checkpoint receptor targets for cancer immunotherapy. Immunol Rev. 2017;276(1):112–20. [PubMed: 28258695]
30. Manieri NA, Chiang EY, and Grogan JL. TIGIT: A Key Inhibitor of the Cancer Immunity Cycle. Trends Immunol. 2017;38(1):20–8. [PubMed: 27793572]
31. Solomon BL, and Garrido-Laguna I. TIGIT: a novel immunotherapy target moving from bench to bedside. Cancer Immunol Immunother. 2018;67(11):1659–67. [PubMed: 30232519]
32. Kurtulus S, Sakuishi K, Ngiow SF, Joller N, Tan DJ, Teng MW, Smyth MJ, Kuchroo VK, and Anderson AC. TIGIT predominantly regulates the immune response via regulatory T cells. J Clin Invest. 2015;125(11):4053–62. [PubMed: 26413872]
33. Chauvin JM, Pagliano O, Fourcade J, Sun Z, Wang H, Sander C, Kirkwood JM, Chen TH, Maurer M, Korman AJ, et al. TIGIT and PD-1 impair tumor antigen-specific CD8(+) T cells in melanoma patients. J Clin Invest. 2015;125(5):2046–58. [PubMed: 25866972]
34. Shen J, Townsend R, You X, Shen Y, Zhan P, Zhou Z, Geng D, Wu D, McGirr N, Soucek K, et al. Pharmacokinetics, pharmacodynamics, and immunogenicity of belatacept in adult kidney transplant recipients. Clin Drug Investig. 2014;34(2):117–26.
35. de Graav GN, Hesselink DA, Dieterich M, Kraaijeveld R, Verschoor W, Roelen DL, Litjens NHR, Chong AS, Weimar W, and Baan CC. Belatacept Does Not Inhibit Follicular T Cell-Dependent B-Cell Differentiation in Kidney Transplantation. Front Immunol. 2017;8(641. [PubMed: 28620390]
36. Amir el AD, Davis KL, Tadmor MD, Simonds EF, Levine JH, Bendall SC, Shenfeld DK, Krishnaswamy S, Nolan GP, and Pe'er D. viSNE enables visualization of high dimensional single-cell data and reveals phenotypic heterogeneity of leukemia. Nat Biotechnol. 2013;31(6):545–52. [PubMed: 23685480]
37. Krummel MF, and Allison JP. CTLA-4 engagement inhibits IL-2 accumulation and cell cycle progression upon activation of resting T cells. J Exp Med. 1996;183(6):2533–40. [PubMed: 8676074]
38. Walunas TL, Bakker CY, and Bluestone JA. CTLA-4 ligation blocks CD28-dependent T cell activation. J Exp Med. 1996;183(6):2541–50. [PubMed: 8676075]
39. Chambers CA, Kuhns MS, Egen JG, and Allison JP. CTLA-4-mediated inhibition in regulation of T cell responses: mechanisms and manipulation in tumor immunotherapy. Annu Rev Immunol. 2001;19(565–94. [PubMed: 11244047]
40. Riley JL. PD-1 signaling in primary T cells. Immunol Rev. 2009;229(1):114–25. [PubMed: 19426218]
41. Francisco LM, Sage PT, and Sharpe AH. The PD-1 pathway in tolerance and autoimmunity. Immunol Rev. 2010;236(219–42. [PubMed: 20636820]
42. Joller N, Hafler JP, Brynedal B, Kassam N, Spoerl S, Levin SD, Sharpe AH, and Kuchroo VK. Cutting edge: TIGIT has T cell-intrinsic inhibitory functions. J Immunol. 2011 ;186(3):1338–42. [PubMed: 21199897]
43. Stengel KF, Harden-Bowles K, Yu X, Rouge L, Yin J, Comps-Agrar L, Wiesmann C, Bazan JF, Eaton DL, and Grogan JL. Structure of TIGIT immunoreceptor bound to poliovirus receptor reveals a cell-cell adhesion and signaling mechanism that requires cis-trans receptor clustering. Proc Natl Acad Sci U S A. 2012;109(14):5399–404. [PubMed: 22421438]
44. de Graav GN, Baan CC, Clahsen-van Groningen MC, Kraaijeveld R, Dieterich M, Verschoor W, von der Thusen JH, Roelen DL, Cadogan M, van de Wetering J, et al. A Randomized Controlled Clinical Trial Comparing Belatacept With Tacrolimus After De Novo Kidney Transplantation. Transplantation. 2017;101(10):2571–81. [PubMed: 28403127]

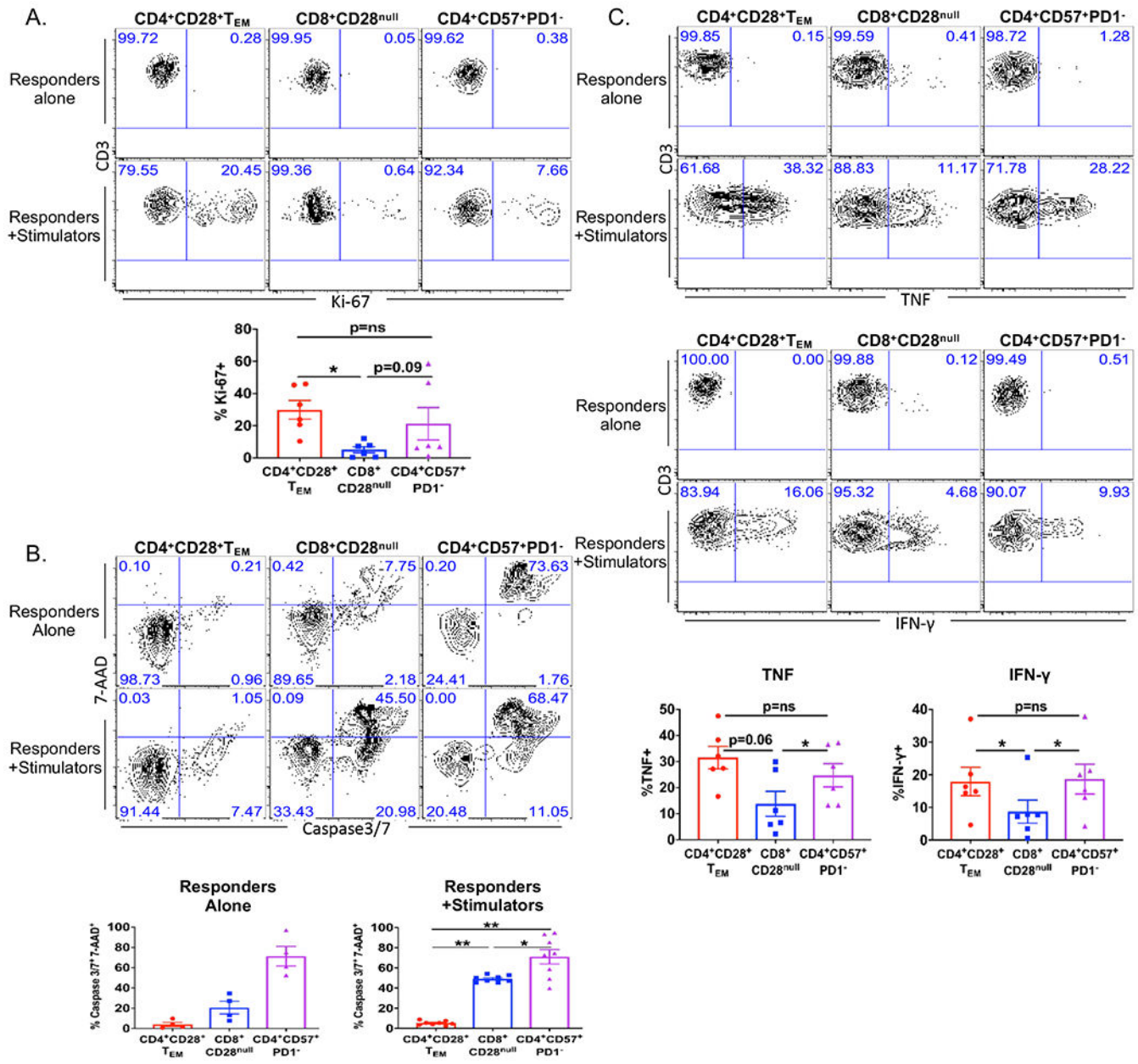

Figure 1. CD4$^+$ CD28$^+$ T$_{EM}$ subset exhibits high proliferative capacity and cytokine functionality and low frequencies of apoptotic cells following stimulation with alloantigen

Responder PBMCs were stimulated in the presence or absence of irradiated, CTV labeled, allogeneic stimulator PBMCs. Risky memory T cell subsets were defined by the following gating strategy: CD4$^+$ CD28$^+$ T$_{EM}$, CD3$^+$ CD4$^+$ CCR7$^-$ CD45RA$^-$ CD28$^+$; CD8$^+$ CD28^{null}, CD3$^+$ CD8$^+$ CD28$^-$; CD4$^+$ CD57$^+$ PD1$^-$, CD3$^+$ CD4$^+$ CD57$^+$ PD1$^-$. (A) Representative flow plots and summary data of frequencies of Ki-67$^+$ proliferating cells within risky memory T cell subsets in the presence or absence of allogeneic stimulation. (*, $p < 0.05$; data depicted are from six independent stimulator/responder pairs). (B) Representative flow plots and summary data of frequencies of Caspase3/7$^+$ 7-AAD$^+$ apoptotic cells within risky memory T cell subsets in the presence or absence of allogeneic stimulation (**, p <

0.01; *, $p < 0.05$; data depicted are from eight independent stimulator/responder pairs). (C) Representative flow plots and summary data of frequencies of TNF-, and IFN-γ-secreting cells within risky memory T cell subsets in the presence or absence of allogeneic stimulation (*, $p < 0.05$; data depicted are from six independent stimulator/responder pairs).

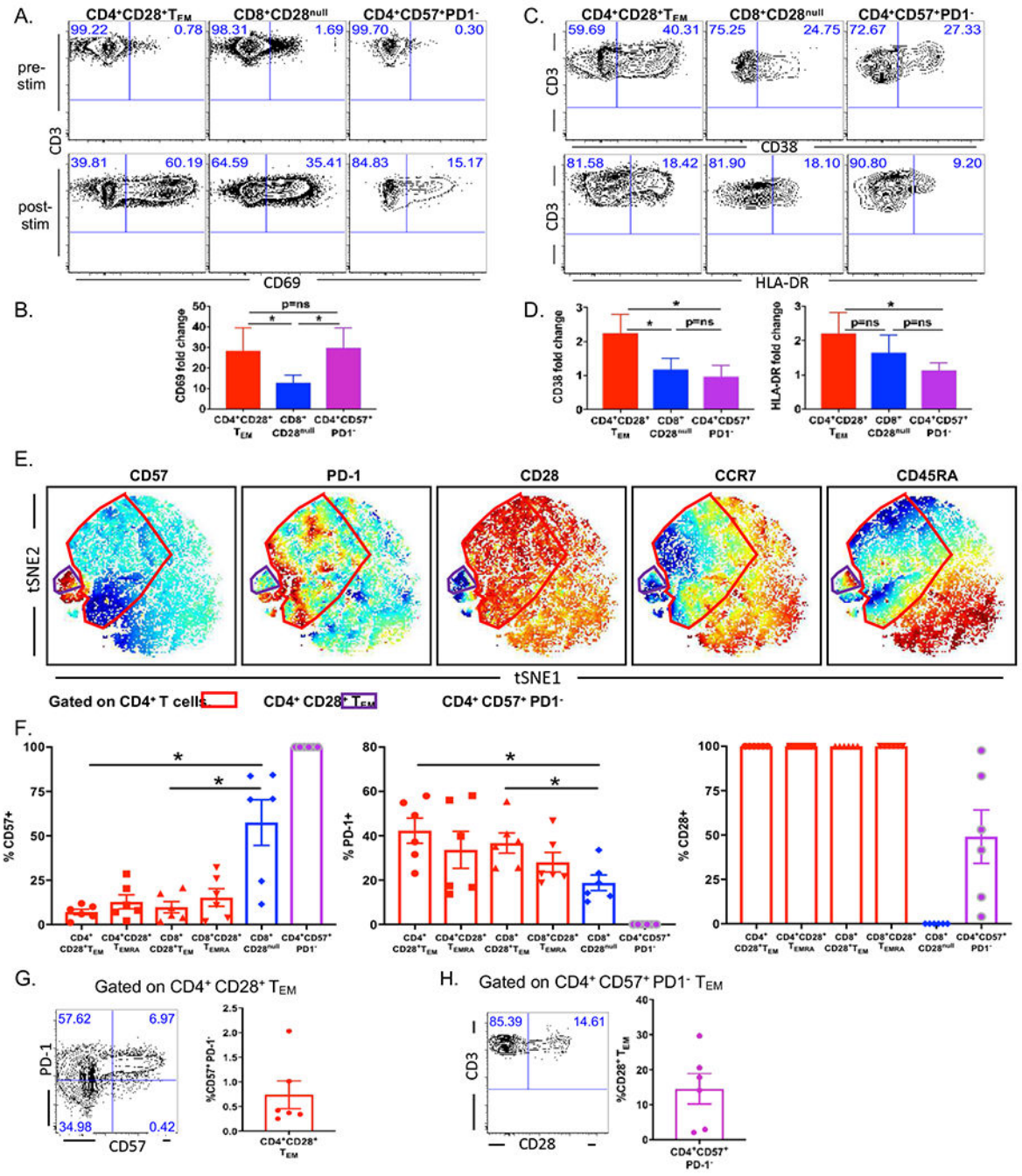

Figure 2. CD4$^+$ CD28$^+$ T_{EM} and CD4$^+$ CD57$^+$ PD1$^-$ subsets exhibit high CD69 upregulation and CD4$^+$ CD28$^+$ T_{EM} exhibit high CD38 and HLA-DR upregulation following stimulation

Human PBMCs from healthy donors were stimulated ex vivo with anti-CD3/CD28 beads for 3 d followed by brief restimulation in the presence or absence of PMA/Iono. PBMCs were analyzed directly ex vivo or following in vitro stimulated as described above by flow cytometry. (A) Representative flow plots of frequencies of CD69$^+$ cells within risky memory T cell subsets pre-(top) and post-(bottom) stimulation. (B) Summary data of fold changes of frequencies of CD69$^+$ cells within risky memory T cell subsets upon stimulation. (C) Representative flow plots of frequencies of CD38$^+$ and HLA-DR$^+$ cells

within risky memory T cell subsets post-stimulation. (D) Summary data of fold changes of frequencies of $CD38^+$ and $HLA\text{-}DR^+$ cells within risky memory T cell subsets upon stimulation. (E) Representative viSNE plots of the median fluorescence intensity (MFI) of CD57, PD-1, CD28, CCR7 and CD45RA within the $CD4^+$ T cell compartment. Red indicates high expression of a given marker, and blue represents low intensity. The red-rimmed population represents $CD4^+$ $CD28^+$ T_{EM} subset, and the purple-rimmed population indicates $CD4^+$ $CD57^+$ $PD1^-$ subset. (F) Summary data of frequencies of $CD57^+$, $PD\text{-}1^+$ and $CD28^+$ cells within risky memory T cell subsets (*, $p < 0.05$; $n = 6$ per experiment; data are representative of three independent experiments. Risky memory T cell subsets were defined by the following gating strategy: $CD4^+$ $CD28^+$ T_{EM}, $CD3^+$ $CD4^+$ $CCR7^-$ $CD45RA^-$ $CD28^+$; $CD8^+$ $CD28^{null}$, $CD3^+$ $CD8^+$ $CD28^-$; $CD4^+$ $CD57^+$ $PD1^-$, $CD3^+$ $CD4^+$ $CD57^+$ $PD1^-$; $CD4^+$ $CD28^+$ T_{EMRA}, $CD3^+$ $CD4^+$ $CCR7^-$ $CD45RA^+$ $CD28^+$; $CD8^+$ $CD28^+$ T_{EM}, $CD3^+$ $CD8^+$ $CCR7^-$ $CD45RA^-$ $CD28^+$; $CD8^+$ $CD28^+$ T_{EMRA}, $CD3^+$ $CD8^+$ $CCR7^-$ $CD45RA^+$ $CD28^+$). G, Frequencies of $CD57^+$ $PD\text{-}1^-$ cells within the $CD4^+$ $CD28^+$ T_{EM} subset. H, Frequencies of $CD28^+$ T_{EM} cells within the $CD57^+$ $PD\text{-}1^-$ subset.

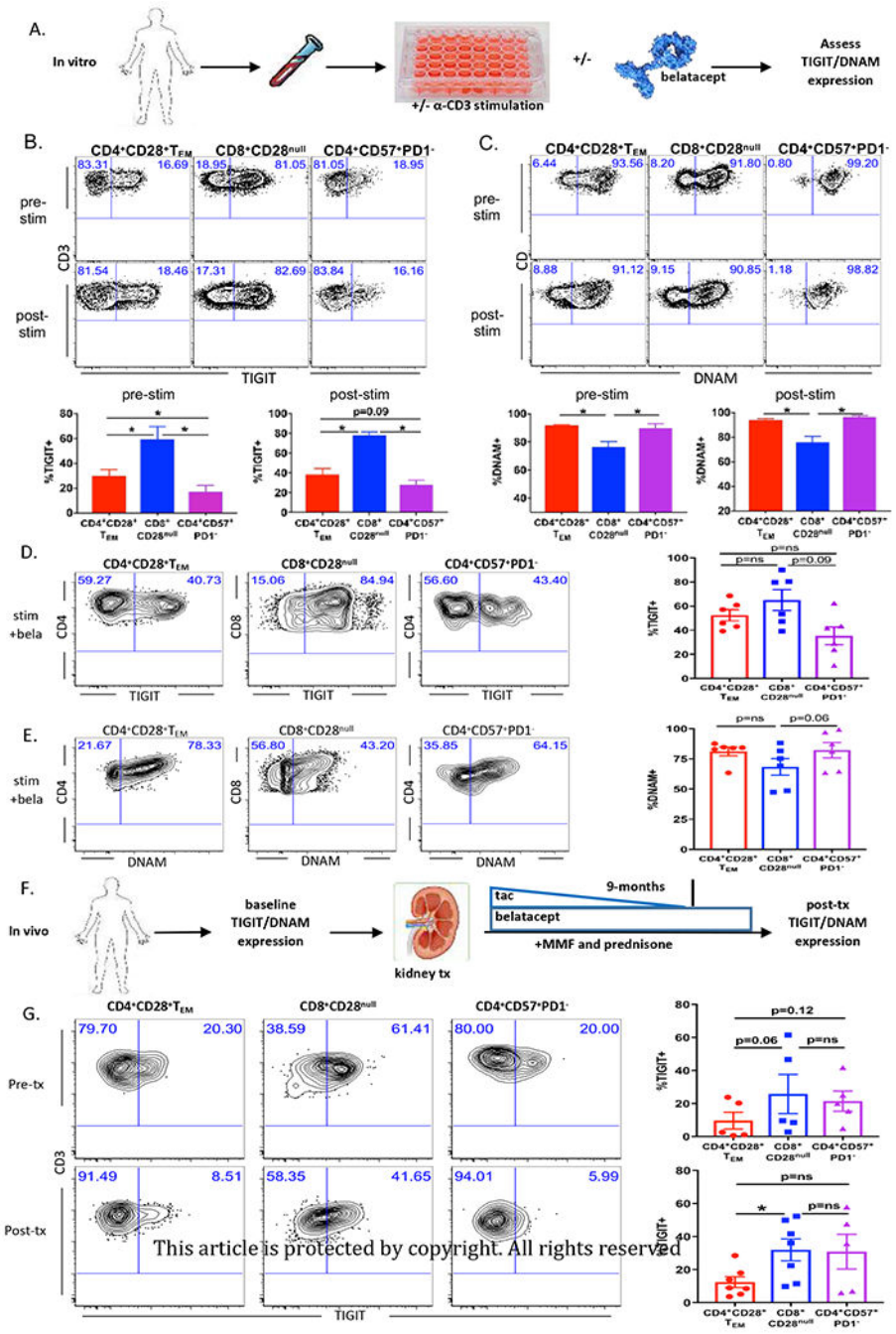

Figure 3. TIGIT expression is maintained on "risky" memory T cell subsets in vivo and in vitro in the presence of belatacept

(A) Schematic of experimental design. Peripheral blood T cells from healthy donors were stimulated ex vivo with anti-CD3 in the presence or absence of belatacept. Risky memory T cell subsets were defined as in Figure 1. Representative flow plots and summary data of frequencies of $TIGIT^+$ cells (B) and $DNAM^+$ cells (C) within risky memory T cell subsets pre- and post-stimulation. TIGIT (D) and DNAM (E) expressions were assessed on risky memory T cell subsets in the setting of belatacept (*, $p < 0.05$; n = 6 per experiment; data are representative of three independent experiments). (F) Schematic of experimental design.

Peripheral T cells from renal transplant patients treated with belatacept as described in (8) were analyzed directly at baseline or following transplantation. (G) TIGIT expression was assessed on risky memory T cell subsets in vivo belatacept-treated transplant patients (*, $p < 0.05$; n = 5-7 per experiment; data are representative of four independent experiments).

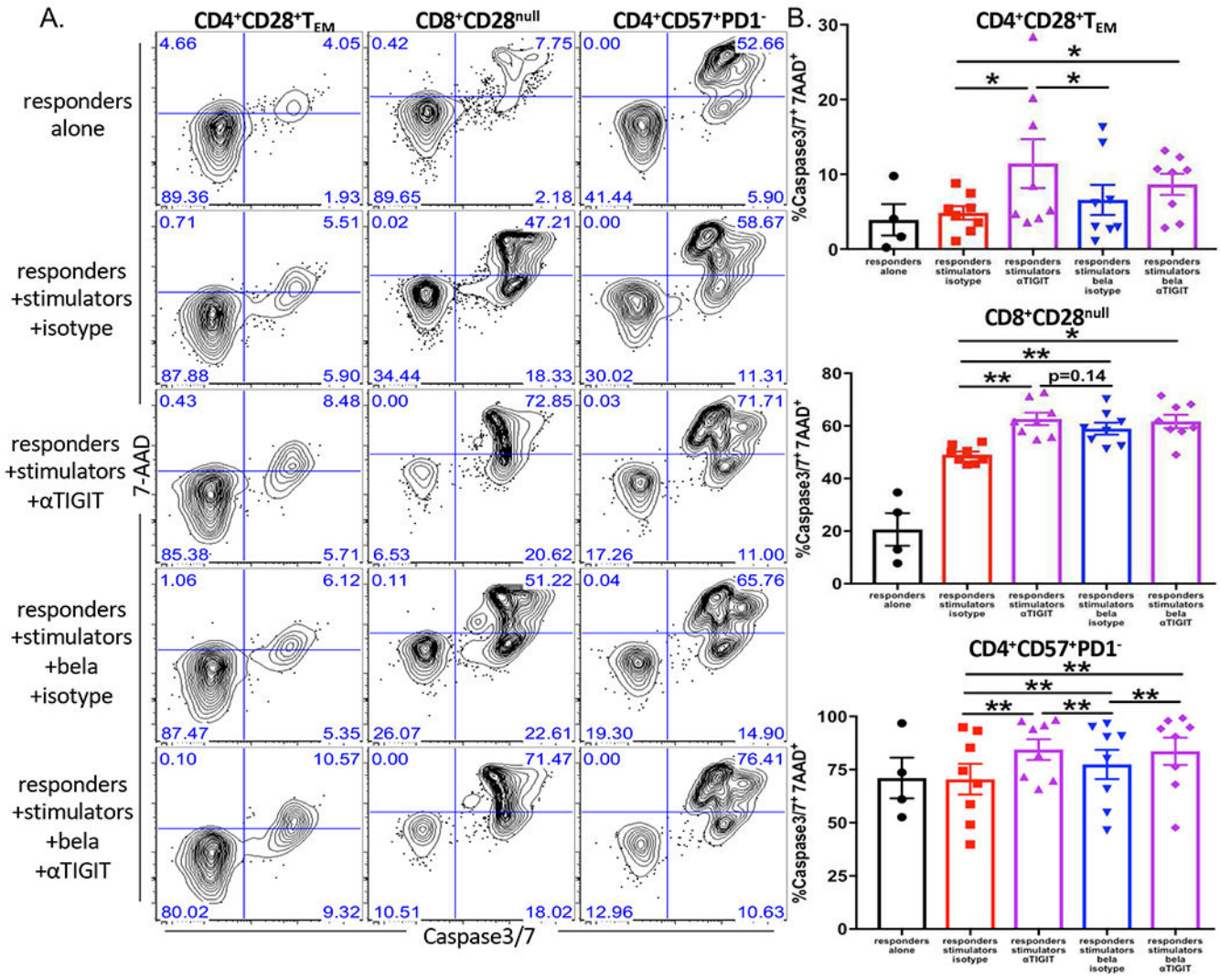

Figure 4. Agonistic αTIGIT induces apoptosis in all three "risky" memory T cell subsets both in the presence and absence of belatacept

Peripheral blood T cells from healthy donors were unstimulated or stimulated ex vivo with allogeneic antigens and treated with agonistic αTIGIT or isotype control in the presence or absence of belatacept. Risky memory T cell subsets were defined as in Figure 1. Representative flow plots (A) and summary data (B) of frequencies of Caspase3/7$^+$ 7-AAD$^+$ apoptotic cells within risky memory T cell subsets (**, $p < 0.01$; *, $p < 0.05$; data depicted are from eight independent stimulator/responder pairs; data are representative of two independent experiments).

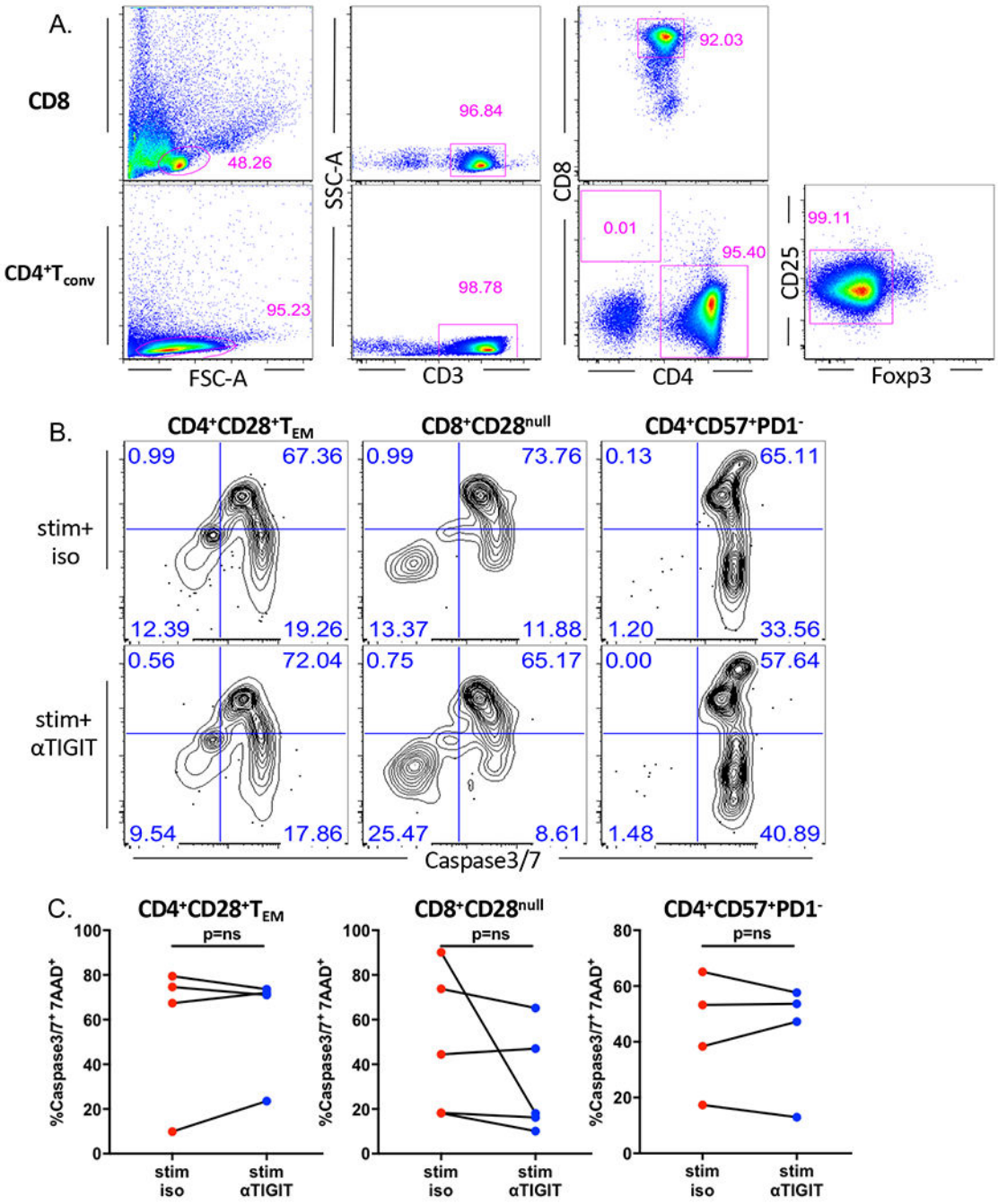

Figure 5. TIGIT-mediated memory T cell apoptosis requires FOXP3$^+$ Treg

CD8$^+$ T cells and CD4$^+$ T$_{conv}$ cells were sorted and stimulated ex vivo with anti-CD3/CD28 beads in the presence of agonistic αTIGIT or isotype control for 3 d. (A) Representative flow plots of the gating strategy to identify sorted CD8$^+$ T cells (top) and CD4$^+$ T$_{conv}$ cells (bottom, CD3$^+$CD4$^+$Foxp3$^-$). (B) Representative flow plots and (C) Summary data of frequencies of Caspase3/7$^+$ 7-AAD$^+$ apoptotic cells within risky memory T cell subsets in

the presence of agonistic αTIGIT or isotype control following ex vivo stimulation (*, $p < 0.05$; n = 4-5 per experiment; data are representative of three independent experiments).